Tuning the Strain and Polymerizability of Organometallic Rings: The Synthesis, Structure, and Ring-Opening Polymerization Behavior of [2]Ferrocenophanes with C−Si, C−P, and C−S Bridges

Rui Resendes,[§] James M. Nelson,[†] Armin Fischer, Frieder Jäkle,[‡] Alexandra Bartole, Alan J. Lough, and Ian Manners*

Contribution from the Department of Chemistry, University of Toronto, 80 St. George Street, Toronto, Ontario M5S 3H6, Canada

Received July 25, 2000

Abstract: A series of novel [2]ferrocenophanes with unsymmetrical C−E bridges has been prepared in which the covalent radius of the second-row element, E, and hence the ring strain present is varied. Species [Fe(η-C_5Me_4)(η-C_5H_4)CH_2ER_x] (**7**, ER_x = $SiMe_2$; **8a**, ER_x = PPh; **8b**, ER_x = PMes; **9**, ER_x = S) were synthesized via reaction of the PMDETA (*N*,*N*,*N*′,*N*″,*N*″-pentamethyldiethylenetriamine) adduct of [(η-C_5H_4Li)Fe(η-C_5Me_4)CH_2Li] with Cl_2ER_x (E = Si or P) or $S(SO_2Ph)_2$. Studies of **7**−**9** by single-crystal X-ray diffraction confirmed the presence of ring-tilted structures: for **7**, α (angle between the planes of the Cp rings) = 11.8(1)°; for **8a**, $\alpha_{average}$ = 14.9(3)°; for **8b**, $\alpha_{average}$ = 18.2(2)°; and for **9**, α = 18.5(1)°. The least tilted compound, **7**, was found to be resistant to thermal, anionic, and transition metal catalyzed ROP. In contrast, the significantly more tilted compounds **8a**, **8b**, and **9** were all found to polymerize thermally with small negative values of ΔH_{ROP} of ca. 10−20 kJ·mol^{-1} determined by DSC. Whereas thermal ROP of **8a** yielded the soluble high molecular weight polycarbophosphaferrocene [(η-C_5Me_4)Fe(η-C_5H_4)CH_2PPh]$_n$ (**11**), species **9** formed the insoluble polycarbothiaferrocene [(η-C_5Me_4)Fe(η-C_5H_4)CH_2S]$_n$ (**14**). Attempted anionic ROP of **8a** and **9** with ^{n}BuLi was unsuccessful and treatment of **8a** with CF_3SO_3Me resulted in the formation of the novel phosphonium salt [(η-C_5Me_4)Fe(η-C_5H_4)CH_2PMePh][CF_3SO_3] (**13**), which was found to be resistant to thermal ROP as a result of its less strained structure (for **13**, α = 11.4(7)°). Treatment of **9** with CF_3SO_3Me or BF_3·Et_2O resulted in the first example of cationic ROP for a transition metal-containing heterocycle to yield polycarbothiaferrocene **14**. In the presence of excess 2,6-di-*tert*-butylpyridine as a selective proton trap, ROP of **9** was only observed with CF_3SO_3Me, and not BF_3·Et_2O, which indicated that Me^+ and H^+ are the probable cationic initiators, respectively. Thermal copolymerization of **9** with trimethylene sulfide resulted in the isolation of the soluble, high molecular weight, random copolymer [(η-C_5Me_4)Fe(η-C_5H_4)CH_2S]$_n$[$(CH_2)_3$S]$_m$, **15**.

Introduction

Macromolecules containing transition metal atoms in the main chain are attracting growing attention as a result of their combination of processability and interesting physical properties.[1,2] Until recently, the development of this area has been hindered by the lack of viable synthetic routes to these materials. As one contribution to the resolution of this problem, the thermal,[3] anionic,[4,5] and transition metal catalyzed[6,7] ring opening polymerization (ROP) of strained [1]ferrocenophanes **1** has been shown to provide a valuable route to a variety of high molecular weight polyferrocenes, **2**. These materials are of fundamental interest as a result of their conformational properties and the presence of interacting metal centers in the main chain and are also attracting attention as semiconductors, charge dissipation coatings, and as precursors to magnetic ceramics and nanostructures.[8−14]

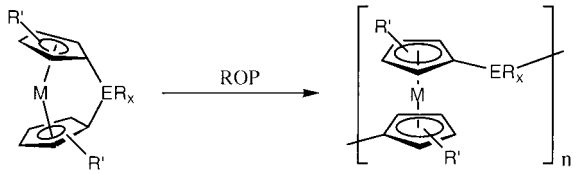

1 **2**

Many [1]ferrocenophanes have been studied crystallographically, and these interesting cyclic organometallic molecules have

[§] Present address: Bayer Inc., Rubber Division, Sarnia, Ontario, Canada.
[†] Present address: 3M Corporate Process Technology Center, St. Paul, MN 55114.
[‡] Present address: Department of Chemistry, Rutgers University, 73 Warren St., Newark, NJ 07102.

(1) Selected recent references: (a) Rosenblum, M. *Adv. Mater*. **1994**, *2*, 159. (b) Puddephatt, R. J. *Chem. Commun.* **1998**, 1055. (c) Chisholm, M. H. *Acc. Chem. Res.* **2000**, *33*, 53. (d) Rehahn, M. *Acta Polym*. **1998**, *49*, 201. (e) Grosche, M.; Herdtweek, E.; Peters, F.; Wagner, M. *Organometallics* **1999**, *18*, 4669. (f) Wolf, M. O.; Zhu, Y. *Adv. Mater*. **2000**, *12*, 599. (g) Pickup, P. G. *J. Mater. Chem*. **1999**, *9*, 1641. (h) Kingsborough, R. P.; Swager, T. M. *Prog. Inorg. Chem*. **1999**, *48*, 123. (i) Nguyen, P.; Gómez-Elipe, P.; Manners, I. *Chem. Rev*. **1999**, *99*, 1515. (j) McAlvin, J. E.; Fraser, C. L. *Macromolecules* **1999**, *32*, 1341. (k) Steffen, W.; Köhler, B.; Altmann, M.; Scherf, U.; Stitzer, K.; Zur Loye, H.-C.; Bunz, U. H. F. *Chem. Eur. J.* **2001**, *7*, 117. (l) Younus, M.; Köhler, A.; Cron, S.; Chawdhury, N.; Al-Mandhary, M. R. A.; Khan, M. S.; Lewis. J.; Long, N. J.; Friend, R. H.; Raithby, P. R. *Angew. Chem., Int. Ed. Engl.* **1998**, *37*, 3036.

(2) Pittman, C. U.; Carraher, C. E.; Zelden, M.; Sheats, J. E.; Culbertson, B. M. *Metal-Containing Polymeric Materials*; Plenum Press: New York, 1996.

(3) Foucher, D. A.; Tang, B.-Z.; Manners, I. *J. Am. Chem. Soc.* **1992**, *114*, 6246.

(4) Ni, Y.; Rulkens, R.; Manners, I. *J. Am. Chem. Soc.* **1996**, *118*, 4102.

(5) Rulkens, R.; Ni, Y.; Manners, I. *J. Am. Chem. Soc.* **1994**, *116*, 12121.

(6) Gómez-Elipe, P.; Resendes, R.; Macdonald, P. M.; Manners, I. *J. Am. Chem. Soc.* **1998**, *120*, 8348.

(7) (a) Ni, Y.; Rulkens, R.; Pudelski, J. K.; Manners, I. *Macromol. Rapid Commun*. **1995**, *16*, 637. (b) Reddy, N. P.; Hayashi, T.; Tanaka, M. *Chem. Commun*. **1995**, 2263.

10.1021/ja002750e CCC: $20.00
Published on Web 02/20/2001

been shown to possess strained, ring-tilted structures in which the cyclopentadienyl (Cp) ligands are tilted by ca. 6−32°, a value defined as the α angle.[15−20] In general, the degree of ring-tilt present in these species is inversely related to the covalent radius of the central atom comprising the bridging unit. Also, density functional calculations indicate that the thermodynamic propensity for these species to undergo ROP reactions is critically dependent on the degree of ring-tilt present.[21,22] However, other factors such as ipso-Cp-bridging atom bond strength and bond polarity also play significant roles in determining the overall reactivity. For example, whereas the highly strained [1]thiaferrocenophane,[23] **1** (M = Fe, ER_x = S, R′ = H) [α = 31°, $\Delta H_{ROP} = -130 \pm 5$ kJ·mol^{-1}], is stable in solution at ambient temperature under an inert atmosphere, under analogous conditions the significantly less strained [1]stannaferrocenophane,[19,24,25] **1** (M = Fe, ER_x = Sn(tBu)$_2$, R′ = H) [α = 14°, $\Delta H_{ROP} = -36 \pm 5$ kJ·mol^{-1}], is more labile and readily undergoes ROP and is challenging to isolate.

The nature of the bridging atom in the monomer also has key implications for the properties of the resulting ring-opened polymers. For example, cyclic voltammetric studies of **2** have revealed the presence of varying Fe···Fe interactions along the polymer main chain which depend on the nature and size of the bridging moiety.[26,27] In the case of polymetallocene **2** (M = Fe, ER_x = S, R′ = Me), the measured redox coupling ($\Delta E_{1/2}$) was found to be 320 mV.[28] This value is significantly larger than the 200−250 mV redox couple found for polyferrocenylsilanes **2** (M = Fe, E = Si). Convincing evidence that these interactions are mediated by the bridge and are not only a function of the Fe···Fe separation has been presented.[24]

While much is now known about [1]ferrocenophanes and their corresponding ring-opened polymers, the analogous chemistry of [2]metallocenophanes is comparatively unexplored.[29] In general, [2]ferrocenophanes would be expected to be less reactive than the analogous [1]ferrocenophanes as a result of the presence of two atoms in the bridge which should lead to a smaller α angle and therefore diminished ring strain. However, we have recently shown that hydrocarbon-bridged monomers such as the [2]ferrocenophanes[30] **3a** and **3b** and the analogous [2]ruthenocenophane, **3c**,[31] possess highly ring-tilted structures (for **3a**, α = 21.6(3)°; for **3c**, α = 29.6(5)°) and undergo thermal ROP to yield the corresponding polymetallocenes, **4a**−**c**. In addition, ring-opening metathesis polymerization of a [2]ferrocenophane with an unsaturated bridge (**3d**) has also been described.[32]

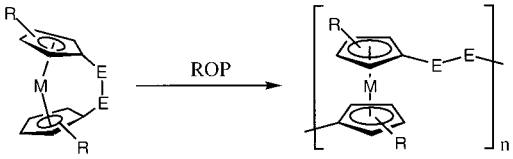

3a: M = Fe, R = H, E_2 = CH_2CH_2
3b: M = Fe, R = Me, E_2 = CH_2CH_2
3c: M = Ru, R = H, E_2 = CH_2CH_2
3d: M = Fe, R = H, E_2 = CH=CH

4a: M = Fe, R = H, E_2 = CH_2CH_2
4b: M = Fe, R = Me, E_2 = CH_2CH_2
4c: M = Ru, R = H, E_2 = CH_2CH_2

In contrast, the corresponding disilane-bridged [2]ferrocenophane, **5a**,[33] and [2]ruthenocenophane, **5b**,[34a] possess structures with significantly less ring-tilt (for **5a**, α = 4.2(2)°; for **5b**, α = 7.8(5)°) and were found to be resistant to ROP. Similarly, the bis(disilane)-bridged [2][2]ferrocenophanes **6a**[34b] and bis(disilane)-bridged [2][2]ruthenocenophane **6b**[34] were found to possess relatively small α angles (for **6a**, α = 7.2(3)°; for **6b**, α = 12.9(2)°) and also do not polymerize.

5a: M = Fe, E = $SiMe_2$
5b: M = Ru, E = $SiMe_2$

6a: M = Fe, E = $SiMe_2$
6b: M = Ru, E = $SiMe_2$

(8) Barlow, S.; Rohl, A. L.; Shi, S.; Freeman, C. M.; O'Hare, D. J. *J. Am. Chem. Soc.* **1996**, *118*, 7578.
(9) MacLachlan, M.; Ginzburg, M.; Coombs, N.; Coyle, T. W.; Raju, N. P.; Greedan, J. E.; Ozin, G. A.; Manners, I. *Science* **2000**, *287*, 1460.
(10) Manners, I. *Chem. Commun.* **1999**, 857.
(11) Massey, J. A.; Power, K. N.; Winnik, M. A.; Manners, I. *Adv. Mater.* **1998**, *10*, 1559.
(12) For the work of other groups on the synthesis of ring-opened polyferrocenes, see, for example: (a) Brandt, P. F.; Rauchfuss, T. B. *J. Am. Chem. Soc*. **1992**, *114*, 1926. (b) Stanton, C. E.; Lee, T. R.; Grubbs, R. H.; Lewis, N. S.; Pudelski, J. K.; Callstrom, M. R.; Erickson, M. S.; McLaughlin, M. L. *Macromolecules*, **1995**, *28*, 8713. (c) Mizuta, T.; Onishi, M.; Miyoshi, K. *Organometallics* **2000**, *19*, 5005. (d) Compton, D. L.; Brandt, P. F.; Rauchfuss, T. B.; Rosenbaum, D. F.; Zukoski, C. F. *Chem. Mater*. **1995**, *7*, 2342. (e) Heo, R. W.; Somoza, F. B.; Lee, T. R. *J. Am. Chem. Soc*. **1998**, *120*, 1621. (f) Brunner, H.; Klankermayer, J.; Zabel, M. *J. Organomet. Chem.* **2000**, *601*, 211. (g) Zürcher, S.; Gramlich, V.; Togni, A. *Inorg. Chim. Acta* **1999**, *291*, 355. (h) Herberhold, M.; Hertel, F.; Milius, W.; Wrackmeyer, B. *J. Organomet. Chem.* **1999**, *582*, 352. (j) Antipin, M. Y.; Vorontsov, I. I.; Dubovik, I. I.; Papkov, V.; Cervantes-Lee, F.; Pannell, K. H. *Can. J. Chem.* **2000**, *78*, 1511.
(13) (a) Pannell, K. H.; Dementiev, V. V.; Li, H.; Cervantes-Lee, F.; Nguyen, M. T.; Diaz, A. F. *Organometallics* **1994**, *13*, 3644. (b) Pannell, K. H.; Robillard, J. U.S. Patent 308856, 1994.
(14) (a) Resendes, R.; Berenbaum, A.; Stojevic, G.; Jäkle, F.; Bartole, A.; Zamanian, F.; Dubois, G.; Hersom, C.; Balmain, K.; Manners, I. *Adv. Mater*. **2000**, *12*, 327. (b) Ginzburg, M.; Galloro, J.; Jäkle, F.; Power-Billard, K. N.; Yang, S.; Sokolov, I.; Lam, C. N. C.; Neumann, A. W.; Manners, I.; Ozin, G. A. *Langmuir* **2000**, *16*, 9609.
(15) Braunschweig, H.; Dirk, R.; Müller, M.; Nguyen, P.; Resendes, R.; Gates, D. P.; Manners, I. *Angew. Chem., Int. Ed. Engl.* **1997**, *36*, 2338.
(16) (a) Broussier, R.; Da Rold, A.; Gautheron, B.; Dromzee, Y.; Jeannin, Y. *Inorg. Chem.* **1990**, *29*, 1817. (b) Bucaille, A.; Le Borgne, T.; Ephritikhine, M.; Daran, J.-C. *Organometallics* **2000**, *19*, 4912. (c) Herberhold, M. *Angew. Chem., Int. Ed. Engl.* **1995**, *34*, 1837.
(17) Butler, I. R.; Cullen, W. R.; Einstein, F. W. B.; Rettig, S. J.; Willis, A. J. *Organometallics* **1983**, *2*, 128.
(18) Osborne, A. G.; Whiteley, R. J. *J. Organomet. Chem.* **1975**, *101*, C27.
(19) Rulkens, R.; Lough, A. J.; Manners, I. *Angew. Chem., Int. Ed. Engl.* **1996**, *35*, 1805.
(20) Seyferth, D.; Withers, H. P. *Organometallics* **1982**, *1*, 1275.
(21) Calculations using density functional theory show that the energy required to tilt the Cp rings is similar to the experimentally determined ΔH_{ROP} value. This indicates that the ring tilting is the most significant factor in determining the thermodynamic tendency of the rings to polymerize. See: Barlow, S.; Drewitt, M. J.; Dijkstra, T.; Green, J. C.; O'Hare, D.; Whittingham, C.; Wynn, H. H.; Gates, D. P.; Manners, I.; Nelson, J. M.; Pudelski, J. K. *Organometallics* **1998**, *17*, 2113.
(22) Green, J. C. *Chem. Soc. Rev.* **1998**, 263.
(23) Pudelski, J. K.; Gates, D. P.; Rulkens, R.; Lough, A. J.; Manners, I. *Angew. Chem., Int. Ed. Engl.* **1995**, *34*, 1506.
(24) Jäkle, F.; Rulkens, R.; Zech, G.; Foucher, D. A.; Lough, A. J.; Manners, I. *Chem. Eur. J.* **1998**, *4*, 2117.
(25) Jäkle, F.; Rulkens, R.; Zech, G.; Massey, J. A.; Manners, I. *J. Am. Chem. Soc.* **2000**, *122*, 4231.
(26) Barlow, S.; O'Hare, D. *Chem. Rev.* **1997**, *97*, 637.
(27) Foucher, D. A.; Honeyman, C. H.; Nelson, J. M.; Tang, B.-Z.; Manners, I. *Angew. Chem., Int. Ed. Engl.* **1993**, *32*, 1709.
(28) Rulkens, R.; Gates, D. P.; Balaishis, D.; Pudelski, J. K.; McIntosh, D. F.; Lough, A. J.; Manners, I. *J. Am. Chem. Soc.* **1997**, *119*, 10976.
(29) For some early examples of [2]ferrocenophanes with hydrocarbon bridges, see: (a) Burke Laing, M.; Trueblood, K. N. *Acta Crystallogr.* **1965**, *19*, 373. (b) Lentzner, H. L.; Watts, W. E. *Tetrahedron* **1971**, *27*, 4343. (c) Yasufuku, K.; Aoki, K.; Yamazaki, H. *Inorg. Chem.* **1977**, *16*, 624.
(30) Nelson, J. M.; Rengel, H.; Manners, I. *J. Am. Chem. Soc.* **1993**, *115*, 7035.
(31) Nelson, J. M.; Lough, A. J.; Manners, I. *Angew. Chem., Int. Ed. Engl.* **1994**, *33*, 989.
(32) Buretea, M. A.; Tilley, T. D. *Organometallics* **1997**, *16*, 1507.

Significantly, the extent of the Fe···Fe interactions in polymetallocenes derived from the ROP of [2]metallocenophanes also appears to be controlled by the nature of the bridging group. Thus, whereas cyclic voltammograms of polyferrocenes **2** (M = Fe, E = Si or S) with a single atom spacer show two reversible redox waves possessing a substantial redox coupling ($\Delta E_{1/2}$) of ca. 250−320 mV, in comparison, the poly(ferrocenylethylene), **4b**, was found to possess a redox couple of only ca. 90 mV, indicating dramatically less electronic communication between adjacent Fe centers.[35,36] This observation is consistent with the more insulating nature of the CH_2CH_2 bridge. Despite the smaller Fe···Fe interactions, oxidized polyferrocenylethylenes show evidence for cooperative magnetic interactions at low temperatures[36] which, in turn, provide a further motivation for the development of related materials.

The ability to synthesize strained [2]ferrocenophanes with variable bridging elements would allow a systematic investigation into the dependence of the covalent radius of the bridging atom on polymerizablity, thus providing insight into the factors that determine the overall reactivity of these interesting molecules. Furthermore, one could, in principle, gain additional control over the degree of electronic communication present along the polymer backbone. With this in mind, we have studied a series of [2]ferrocenophanes, **7**−**9**, in which the covalent radius of one of the bridging elements is varied (for **7**, Si: $r_{cov} = 1.17$ Å; for **8**, P: $r_{cov} = 1.10$ Å; for **9**, S: $r_{cov} = 1.04$ Å).[37] In this paper, we report on the syntheses, characterization, and comparative polymerization behavior of these interesting, unsymmetrically bridged species.

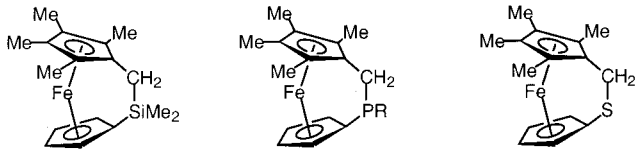

7 **8a:** R = Ph **8b:** R = Mes **9**

Results and Discussion

As exemplified by work on the polymerizable hydrocarbon-bridged species **3a**, **3b**, and **3d** and the polymerization resistant compound **5a**, there have been several previous studies of the ROP behavior of symmetrically bridged [2]ferrocenophanes. However, the development of [2]ferrocenophanes with unsymmetrical bridging units is virtually unexplored and, to our knowledge, no ROP studies have been reported. Previous work by Abramovitch et al. involved the synthesis of the S−N bridged [2]thiazaferrocenophane, **10a**, through the photolysis of ferrocenesulfonyl azide.[38] Subsequent characterization of this species revealed the presence of a significantly ring-tilted structure ($\alpha = 23°$). Several years later, Wrighton and co-workers reported the synthesis of the first carbosila-bridged [2]ferrocenophane, **10b**, via the reaction of pentamethylferrocene (Cp*FeCp, Cp* = C_5Me_5) with ^{n}BuLi in the presence of PMDETA (*N*,*N*′,*N*″,*N*″-pentamethyldiethylenetriamine) followed by the addition of $SiCl_4$.[39] This route appeared potentially attractive to us as the introduction of different bridging elements into this unsymmetrical [2]ferrocenophane template appeared to be possible. In this paper we discuss the use of this approach to generate a series of novel [2]ferrocenophanes possessing C−Si, C−P, and C−S bridges.

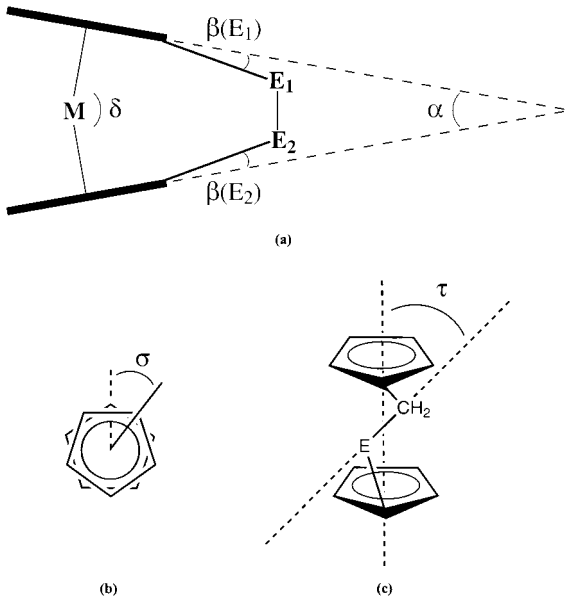

Figure 1. Definitions of angles found in a [2]metallocenophane framework: (a) α, β, and δ, (b) staggering angle, σ, and (c) torsional angle, τ.

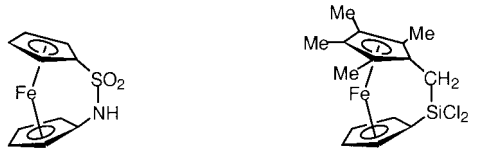

10a **10b**

1. Synthesis and Spectroscopic Characterization of [2]Ferrocenophanes 7−9. The [2]ferrocenophanes, **7**−**9**, were successfully synthesized in 26−56% yields via the reaction of the PMDETA adduct of [(η-C_5H_4Li)Fe(η-C_5Me_4)CH_2Li] with a slight excess of the appropriate main group reagent (Cl_2SiMe_2, Cl_2PPh, Cl_2PMes, or $S(SO_2Ph)_2$). The identity of each species was confirmed by ^{1}H and ^{13}C NMR, elemental analysis, and, where applicable, also by ^{29}Si and ^{31}P NMR and by mass spectrometry.

Previous work has shown that the ^{13}C NMR resonance of the ipso-Cp carbon atom bonded to the bridging atom of strained [1]ferrocenophanes is shifted to higher fields as a consequence of the structural distortion imposed at the ipso-Cp carbon atom by the bridging moiety.[24,28,40] Furthermore, the extent of the

(33) Finckh, W.; Tang, B.-Z.; Foucher, D.; Zamble, D. B.; Ziembinski, R.; Lough, A.; Manners, I. *Organometallics* **1993**, *12*, 823.

(34) (a) Nelson, J. M.; Lough, A. J.; Manners, I. *Organometallics* **1994**, *13*, 3703. (b) Jutzi, P.; Krallmann, R.; Wolf, G.; Neumann, B.; Stammler, H.-G. *Chem. Ber.* **1991**, *124*, 2391. (c) A Ge−Ge bridged [2]ferrocenophane has been reported to undergo metal-catalyzed ROP: Mochida, K.; Shibayama, N.; Goto, M. *Chem. Lett.* **1998**, 339. We presume that the weaker bonds involving Ge are a key factor.

(35) (a) Foucher, D. A.; Honeyman, C. H.; Nelson, J. M.; Tang, B.-Z.; Manners, I. *Angew. Chem., Int. Ed. Engl.* **1993**, *32*, 1709. (b) Rulkens, R.; Lough, A. J.; Manners, I.; Lovelace, S. R.; Grant, C.; Geiger, W. E. *J. Am. Chem. Soc.* **1996**, *118*, 12683.

(36) Nelson, J. M.; Nguyen, P.; Petersen, R.; Rengel, H.; Macdonald, P. M.; Lough, A. J.; Manners, I.; Raju, N. P.; Greedan, J. E.; Barlow, S.; O'Hare, D. *Chem. Eur. J.* **1997**, *3*, 573.

(37) Wells, A. F. *Structural Inorganic Chemistry*, 5th ed.; Oxford University Press: New York, 1984.

(38) Abramovitch, R. B.; Atwood, J. L.; Good, M. L.; Lampert, B. A. *Inorg. Chem.* **1975**, *14*, 3085.

(39) Chao, S.; Robbins, J. L.; Wrighton, M. S. *J. Am. Chem. Soc.* **1983**, *105*, 181. For a recent report of a Si-Ge bridged [2]ferrocenophane see Sharma, S.; Caballero, N.; Li, H.; Pannell, K. H. *Organometallics* **1999**, *18*, 2855.

(40) Osborne, A. G.; Whiteley, R. H.; Meads, R. E. *J. Organomet. Chem.* **1980**, *193*, 345.

upfield shift can be taken as an indication of the overall ring strain (as indicated by the β angle, see Figure 1) present in the system. For compounds **7**, **8a**, **8b**, and **9** the ^{13}C NMR resonances due to the ipso-Cp-E carbons were found to occur at 70.5, 74.7, 79.4, and 93.7 ppm (in C_6D_6), respectively. These values occur at much lower fields than those typically found for the analogous [1]ferrocenophanes (for **1**, M = Fe, ER_x = $SiMe_2$, R′ = H and $\delta_{ipso-Cp}$ = 33.5 ppm; for **1**, M = Fe, ER_x = PPh, R′ = H and $\delta_{ipso-Cp}$ = 18.6 ppm; for **1**, M = Fe, ER_x = S, R′ = H and $\delta_{ipso-Cp}$ = 14.3 ppm (all in C_6D_6)) and are similar to those for acyclic analogues which suggests that compounds **7**−**9**, as expected, possess significantly less strained structures. The appreciably downfield shifted resonance due to the ipso-Cp-S carbon of **9** (cf. **7**, **8a**, and **8b**) is also consistent with previous work by Rauchfuss and co-workers who have reported that the analogous ipso-Cp carbon resonances of 1,1′-trithia[3]ferrocenophanes occur in the range 98.5−87.6 ppm.[41−43]

The ^1H NMR spectra of **7** and **9** revealed the presence of two pseudotriplets (for **7**, δ = 4.12 and 3.95 ppm; for **9**, δ = 4.69 and 3.64 ppm) assigned to the α and β protons of the unsubstituted Cp ring. The splitting between the pseudotriplets of **7** ($\Delta\delta$ = 0.17 ppm) is much less pronounced than that observed for the analogous [1]ferrocenophane (**1**, M = Fe, ER_x = $SiMe_2$, R′ = H and $\Delta\delta$ = 0.40 ppm) which, based on previous interpretations, suggests that **7** is significantly less strained than the corresponding [1]ferrocenophane.[33] However, the splitting between the pseudotriplets of **9** ($\Delta\delta$ = 1.05 ppm) is significantly greater than that found for the corresponding [1]ferrocenophane (**1**, M = Fe, ER_x = S, R′ = H and $\Delta\delta$ = 0.65 ppm), which indicates that such $\Delta\delta$ measurements are an unreliable indication of strain in metallocenophanes. Unlike **7** and **9**, the [2]ferrocenophanes **8a** and **8b** possess unsymmetrical bridging moieties and therefore exhibit four unique Cp resonances in both the ^1H and ^{13}C NMR spectra. Of particular interest in the ^1H NMR spectra of **8a** and **8b** are the CH_2 resonances of the bridging moiety, each of which occur as a doublet of doublets due to $^2J_{PC}$ coupling and geminal J_{HH} coupling.

Previous studies on [1]- and [2]ferrocenophanes have demonstrated that the absorption maximum attributed to the lowest energy d−d transition is shifted to a longer wavelength when compared to analogous unstrained species.[28,40] Furthermore, the extent of the bathochromic shift was found to be mainly dependent on the α angle and theoretical calculations on [1]ferrocenophanes have shown that the HOMO-LUMO energy gap decreases as the α angle increases.[21,28,44] To further probe the degree of ring strain present in compounds **7**−**9**, UV/visible spectra were obtained (in hexanes) in the region of 250−800 nm and the results are compiled in Table 1. The UV/visible spectrum of **7** shows an absorption maximum at 458 nm (ϵ = 120 M^{-1} cm^{-1}) for the lowest energy d−d transition, which is significantly bathochromically shifted when compared to pentamethylferrocene (λ_{max} = 430 nm, ϵ = 120 M^{-1} cm^{-1}) and the unbridged compound (η-$C_5H_4SiMe_3)_2Fe$ (λ_{max} = 448 nm, ϵ = 132 M^{-1} cm^{-1}). This suggests an appreciably ring-tilted structure for **7**. The UV/visible spectra of **8a** and **8b** reveal analogous absorptions at 472 (ϵ = 280 M^{-1} cm^{-1}) and 465 nm (ϵ = 310 M^{-1} cm^{-1}), respectively. The individual absorption maxima also occur at longer wavelengths compared to pentamethylferrocene and the bathochromic shifts are more pronounced than that observed for **7**, suggesting that compounds **8a** and **8b** possess more highly tilted and hence more highly strained structures. The UV/visible spectrum of **9** revealed a corresponding absorption maximum at 475 nm (ϵ = 240 M^{-1} cm^{-1}) and a slightly greater bathochromic shift than that of **8a** compared to pentamethylferrocene. These observations tentatively suggest that the α angle significantly increases as the bridging element in the [2]ferrocenophane framework is changed from silicon, to phosphorus, to sulfur, which is consistent with the decreasing covalent radius accompanying this series of second-row elements.

Table 1. UV/Vis λ_{max} Values and Redox Couples (Referenced to the Ferrocene/Ferrocenium Ion Couple) for Compounds **7**−**9**

compd	λ_{max} (nm)[a]	ϵ (M^{-1} cm^{-1})[a]	$E_{1/2}$ (mV)[b]
(η-C_5Me_5)(η−C_5H_5)Fe	430	120	−289
7	458	120	−304
8a	472	280	−133
8b	465	310	
9	475	240	−102
13	465[c]	120	370
(η-$C_5H_5)_2Fe$	440	90	0

[a] In hexanes. [b] In CH_2Cl_2. [c] In THF.

2. X-ray Structural Analysis of [2]Ferrocenophanes 7−9. To examine the degree of ring strain present in the [2]ferrocenophanes **7**−**9** in detail, single-crystal X-ray analysis was performed for each species. Figure 1 depicts the various angles as found in the [2]metallocenophane framework, including the torsional and staggering angles σ and τ.

Suitable single crystals of **7** were obtained by sublimation under high vacuum at 80 °C while suitable single crystals for **8a**, **8b**, and **9** were obtained from low-temperature recrystallization (−30 °C) from minimal MeCN (**8a** and **8b**) and hexanes (**9**). The molecular structures of compounds **7**−**9** are shown in Figures 2−5. Unit cell parameters are given in Table 2 and comparative bond angles, including torsional and staggering angles, are shown in Table 3.

Examination of the molecular structures of compounds **7**−**9** revealed the presence of significant α angles ranging from 11.8(1)° to 18.5(1)°. The CH_2−$SiMe_2$ bridged [2]ferrocenophane (**7**) was found to possess the smallest α angle at 11.8(1)°, consistent with the observation that the λ_{max} value observed in the UV/visible spectrum of this species was the least bathochromically shifted relative to pentamethylferrocene.

Crystals of the CH_2−PPh and CH_2−PMes bridged [2]ferrocenophanes (**8a** and **8b**) were both found to possess two independent molecules in the unit cell. The average α angles were surprisingly found to be significantly different in the solid state, with values of 14.9(3)° and 18.2(2)° for **8a** and **8b**, respectively. This observation contradicts the prediction from the UV/visible data obtained for these compounds in solution, which suggests that **8a** is slightly more strained. However, also noteworthy is the difference in the total β angle contribution ($\beta(E_1) + \beta(E_2)$), which for **8a** is 26.8(4)° and for **8b** is 23.5(3)° in the solid state. Careful examination of the crystal packing diagrams for compounds **8a** and **8b** provided insight into the factors which may account for the structural differences. Unlike the phenyl substituents on the phosphorus centers of **8a**, the mesityl groups of **8b** were found to π-stack with neighboring mesityl units in the solid state (Figure 4b). This appears to lead to a preference for a slightly (ca. 3°) greater α angle and a smaller (ca. 3°) β-angle contribution in **8b** relative to **8a**.

X-ray diffraction analysis of **9** also revealed a strained molecular structure consistent with the UV/visible spectrum.

(41) Compton, D. L.; Rauchfuss, T. B. *Organometallics* **1994**, *13*, 4367.
(42) Brandt, P. F.; Compton, D. L.; Rauchfuss, T. B. *Organometallics* **1998**, *17*, 2702.
(43) Davison, A.; Smart, J. C. *J. Organomet. Chem.* **1979**, *174*, 321.
(44) The HOMO-LUMO gap is also slightly modified by the nature of the bridging element; see: Berenbaum, A.; Braunschweig, H.; Dirk, R.; Englert, U.; Green, J. C.; Jäkle, F.; Lough, A. J.; Manners, I. *J. Am. Chem. Soc.* **2000**, *122*, 5765.

Table 2. Summary of Selected Crystal Data for [2]Ferrocenophanes **7**−**9** and **13**

	7 $E_1 = CH_2$ $E_2 = SiMe_2$	**8a** $E_1 = CH_2$ $E_2 = PPh$	**8b** $E_1 = CH_2$ $E_2 = PMes$	**9** $E_1 = CH_2$ $E_2 = S$	**13** $E_1 = CH_2$ $E_2 = [PMePh]^+$
emp. formula	$C_{17}H_{24}FeSi$	$C_{21}H_{23}FeP$	$C_{24}H_{29}FeP$	$C_{15}H_{18}FeS$	$C_{23}H_{26}F_3FeO_3PS$
M_r	312.3	362.2	404.3	286.2	526.3
cryst. class	triclinic	triclinic	monoclinic	monoclinic	monoclinic
space group	$P\bar{1}$	$P\bar{1}$	$P2(1)/c$	$P2(1)/c$	$C2/c$
a, Å	7.347(1)	10.6721(11)	8.4879(3)	8.0787(6)	25.8739(1)
b, Å	8.464(1)	13.2867(9)	27.4428(11)	24.179(3)	6.7719(3)
c, Å	14.190(1)	14.1653(15)	17.3725(4)	7.5462(10)	27.7679(16)
α, deg	74.90(1)	71.687(5)	90	90	90
β, deg	89.57(1)	70.138(4)	91.899(2)	117.5	109.336(2)
γ, deg	66.41(1)	69.365(6)	90	90	90
Z	2	4	8	4	8
D_{cal}, g·cm^{-3}	1.336	1.395	1.328	1.455	1.523
GOF	1.065	0.922	0.959	1.139	1.028
$R1[1 > 2\alpha(I)]$	0.0426	0.0534	0.0480	0.0365	0.0607
w$R2$[all data]	0.1117	0.1104	0.1087	0.0975	0.1330

Table 3. Comparative Angles for [2]Ferrocenophanes **3a**, **5a**, **7**−**9**, and **13**

	compd	α (deg)	δ (deg)	$\beta(E_1)$ (deg)	$\beta(E_2)$ (deg)	σ (deg)[b]	τ (deg)[a]	ref
3a	$E_1 = CH_2$ $E_2 = CH_2$	21.6(3)	164.1(3)	21.4(3)	13.3(3)	1.2(2)	18.0(5)	36
5a	$E_1 = SiMe_2$ $E_2 = SiMe_2$	4.19(2)	176.5(3)	10.8(3)	10.8(3)	6.0(1)	8.4(4)	33
7	$E_1 = CH_2$ $E_2 = SiMe_2$	11.8(1)	170.9(14)	7.3(3)	17.9(3)	0.1(2)	0.5(2)	*c*
8a[1]	$E_1 = CH_2$ $E_2 = PPh$	14.8(3)	169.7(2)	9.8(4)	18.0(4)	11.0(3)	21.7(3)	*c*
8a[2]	$E_1 = CH_2$ $E_2 = PPh$	15.0(4)	169.6(2)	11.1(4)	14.7(4)	14.5(3)	30.0(3)	*c*
8b[1]	$E_1 = CH_2$ $E_2 = PMes$	18.1(2)	167.6(1)	13.7(3)	9.8(3)	16.7(2)	29.5(2)	*c*
8b[2]	$E_1 = CH_2$ $E_2 = PMes$	18.3(2)	167.2(1)	14.0(3)	9.4(3)	15.3(2)	29.4(2)	*c*
9	$E_1 = CH_2$ $E_2 = S$	18.5(1)	167.2(1)	9.3(2)	10.6(2)	10.0(2)	17.9(3)	*c*
13	$E_1 = CH_2$ $E_2 = PMePh$	11.4(7)	172.2(2)	10.5(4)	18.6(3)	3.1(1)	8.9(1)	*c*

[a] τ = torsional angle; angle between the bridging E−E bond and the plane containing the Cp centroids and the Fe atom. [b] σ = staggering angle; angle with which the Cp rings deviate from the eclipsed conformation. [c] Results obtained from this study.

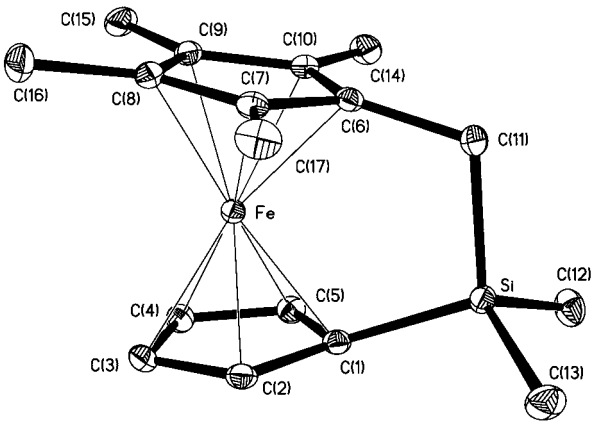

Figure 2. Molecular structure of **7** showing 30% thermal ellipsoids.

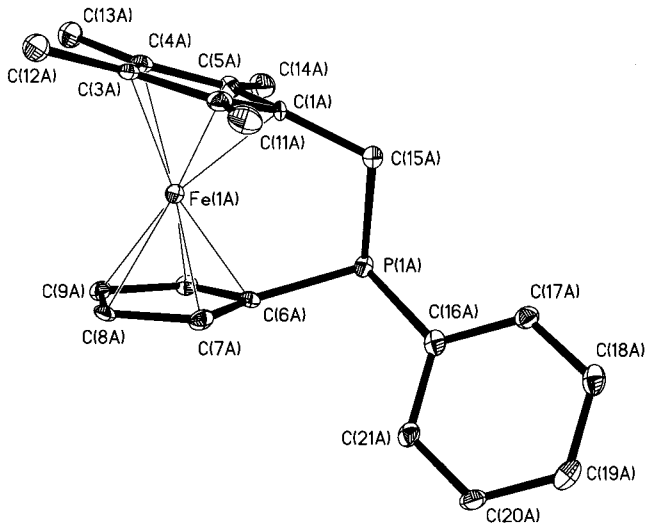

Figure 3. Molecular structure of **8a** showing 30% thermal ellipsoids. Two molecules were found in the unit cell; for clarity only the A molecule is shown.

The observed α angle of 18.5(1)° is the largest found for the [2]ferrocenophanes studied in this work, and is consistent with the fact that sulfur possesses the smallest covalent radius of all the bridging elements used in this study. It is noteworthy that the α angle found for **9** is, however, similar to that found for **8b** (18.2(2)°) (Table 3). Furthermore, the total β angle contribution in **9** is significantly less (19.9(2)° versus 23.5(3)° for **8b**). Significantly, whereas four Cp resonances are noted in the ^{1}H and ^{13}C NMR spectra of **8a** and **8b** only two are detected in the case of **9**; the C−S bridge in the latter species must be stereochemically nonrigid on the NMR time scale at 25 °C.

3. Cyclic Voltammetric Studies of [2]Ferrocenophanes 7−**9.** Previous work has shown that most [1]ferrocenophanes

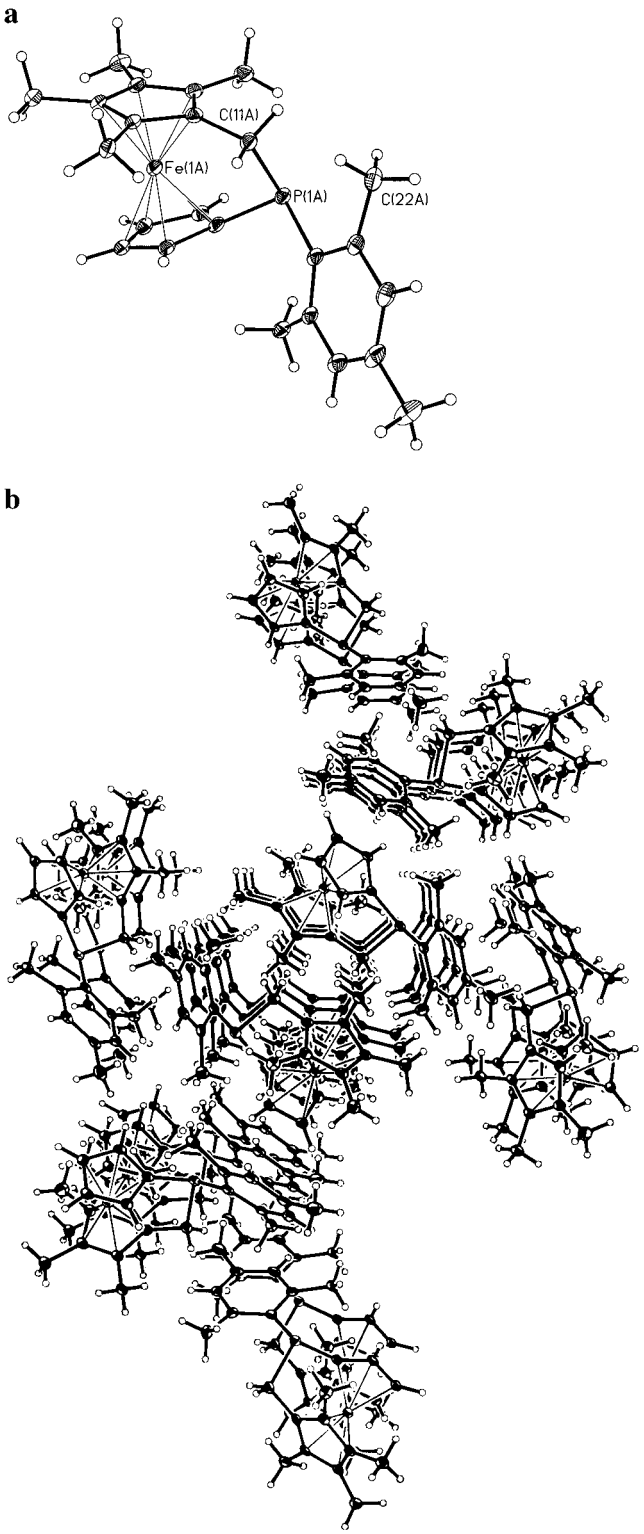

Figure 4. (a) Molecular structure of **8b** (A molecule) showing 30% thermal ellipsoids and hydrogen atoms. For clarity, some of the atomic labels have been omitted. (b) Packing diagram for **8b**.

undergo reversible one-electron oxidation processes.[45] However, in the case of very highly strained species (e.g. **1**, M = Fe, ER_x = S, R′ = H) the process appears to be irreversible.[28]

Cyclic voltammetric studies of compounds **7**−**9** in a 0.1 M solution of $[NBu_4][PF_6]$ in CH_2Cl_2 revealed these species to also possess chemically reversible redox couples ranging from $E_{1/2} = -304$ to -102 mV (versus the ferrocene/ferrocenium ion couple) (Table 1). The observed redox couples were found centered at more negative potentials than that observed for ferrocene consistent with the more electron-rich iron center in these species arising from the presence of a tetramethylated-Cp ligand. A plot of current versus the (scan rate)$^{1/2}$ for each compound measured was linear, indicating that the redox process was diffusion limited.

The measured redox couples were found to shift to more positive potentials (versus ferrocene/ferrocenium) as the electronegativity of the bridging element E increased. Similar observations have been made for [1]ferrocenophanes.[28,46]

4. Polymerization Behavior of [2]Ferrocenophanes 7−9. The spectroscopic and crystallographic characterization of the [2]ferrocenophanes, **7**−**9**, suggests that these species possess varying degrees of ring strain (indicated in part by the α angle). As a result, these species were viewed as potential candidates for ROP. Furthermore, by analyzing and comparing the polymerization behavior of **7**−**9**, we anticipated being able to examine the α angle dependence on the polymerizability of [2]ferrocenophanes in a controlled manner for the first time.

(i) Polymerization Behavior of the [2]Carbosilaferrocenophane 7. Attempts to thermally polymerize **7** involved heating this species in the melt in a sealed, evacuated Pyrex tube at 150 to 350 °C for up to 7 days. However, no increase in melt viscosity was detected in any experiment and analysis of the tube contents by ^{1}H NMR (in $CDCl_3$) showed only unreacted **7**. Subsequent analysis of the tube contents by GPC in THF showed that no high molecular weight material (M_w > 1000 g·mol^{-1}) was present. As the thermal polymerization of **7** was unsuccessful, anionic ring-opening methods, previously reported for silicon-bridged [1]ferrocenophanes[4,5] and cyclic tetrasilanes,[47] were also investigated. However, attempts to induce ROP by the addition of small or equimolar amounts of such anionic initiators as ^{n}BuLi or PhLi to THF solutions of **7** were unsuccessful. Additionally, treatment of **7** in the melt at 150−160 °C with a small quantity of $K[OSiMe_3]$ resulted in no detectable polymerization. The use of transition metal precatalysts such as $[(cyclooctene)_2RhCl]_2$ also proved unsuccessful. In all cases, only unreacted **7** was detected by ^{1}H NMR analysis and mass spectrometry. Subsequent analysis of the reaction mixtures by GPC confirmed that no ROP had occurred. The resistance of **7** toward polymerization suggests that this species does not possess sufficient ring strain to undergo ROP.

(ii) Polymerization Behavior of the [2]Carbophosphaferrocenophanes 8a,b. Differential scanning calorimetry (DSC) analysis of **8a** and **8b** revealed endotherms associated with the respective melting points at 88 and 105 °C. In addition, small broad exotherms at 256 ($\Delta H_{ROP} = -12 \pm 5$ kJ·mol^{-1}) and 287 °C ($\Delta H_{ROP} = -21 \pm 5$ kJ·mol^{-1}) characteristic of ROP processes were detected (Figure 6). Due to the relative ease associated with the synthesis of **8a** compared to **8b**, the remainder of the polymerization studies focused on **8a**.

When a sample of **8a** was heated in a sealed, evacuated Pyrex tube at 220−250 °C, a viscosity increase was observed after a 6 h period. After extraction of the tube contents into THF followed by precipitation into hexanes, a yellow-fibrous material (**11**) was obtained (Scheme 1). ^{1}H, ^{13}C, and ^{31}P NMR (in C_6D_6) analysis of this material confirmed the assigned structure. Of note in the ^{1}H NMR spectrum of **11** are the broad resonances

(45) Pudelski, J. K.; Foucher, D. A.; Honeyman, C. H.; Lough, A. J.; Manners, I.; Barlow, S.; O'Hare, D. *Organometallics* **1995**, *14*, 2470.

(46) Peckham, T. J.; Lough, A. J.; Manners, I. *Organometallics* **1999**, *18*, 1030.

(47) (a) Cypryk, M.; Gupta, Y.; Matyjaszewski, K. *J. Am. Chem. Soc.* **1991**, *113*, 1046. (b) Fossum, E.; Matyjaszewski, K. *Macromolecules* **1995**, *28*, 1618.

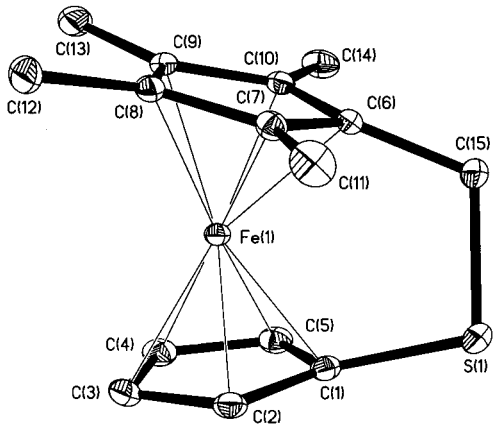

Figure 5. Molecular structure of **9** showing 30% thermal ellipsoids.

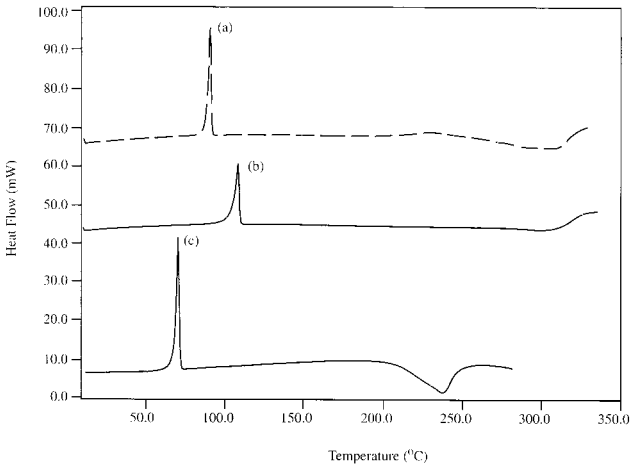

Figure 6. DSC traces of (a) **8a**, (b) **8b**, and (c) **9**: for **8a**, 5.0 mg; for **8b**, 7.4 mg; and for **9**, 3.5 mg. Heating rate 10 °C/min.

Scheme 1

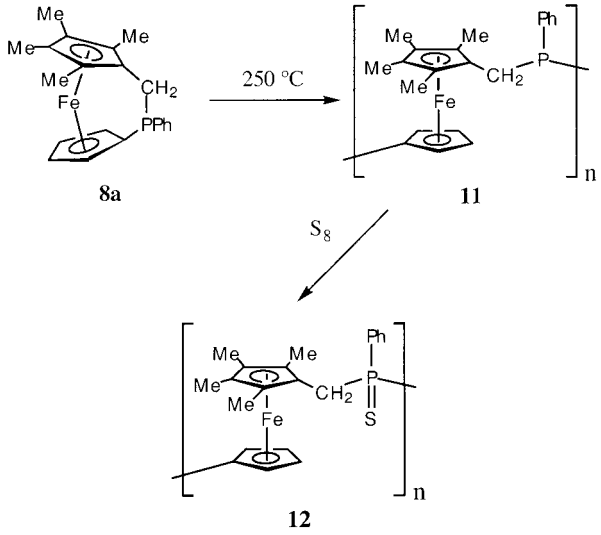

occurring between 7.42 and 7.02, 3.93 and 3.67, 3.22 and 3.10, and 2.21 and 1.26 ppm due to the Ph, Cp, CH_2, and Me protons of **11**, respectively (Figure 7). The ^{31}P NMR of **11** revealed a significantly upfield shifted ^{31}P NMR resonance compared to the monomer, **8a** (for **11**, $\delta(^{31}P, C_6D_6) = -31.7$ ppm; for **8a**, $\delta(^{31}P, C_6D_6) = 7.5$ ppm), consistent with that observed when the analogous phosphorus-bridged [1]ferrocenophane, **1** (M = Fe, ER_x = PPh, R′ = H and $\delta(^{31}P, C_6D_6) = 13.0$ ppm), is polymerized to form the corresponding poly(ferrocenylphosphine) **2** (M = Fe, ER_x = PPh, R′ = H and $\delta(^{31}P, C_6D_6) = -31.7$ ppm).[48] The UV/visible spectrum of **11** (in THF), in the region of 250−800 nm, shows an absorption at 443 nm (ϵ = 148 M^{-1} cm^{-1}) for the lowest energy d−d transition. The shift in λ_{max} to shorter wavelengths, as compared to **8a** (λ_{max} = 472 nm), is consistent with the relief of ring strain accompanying ROP.[21]

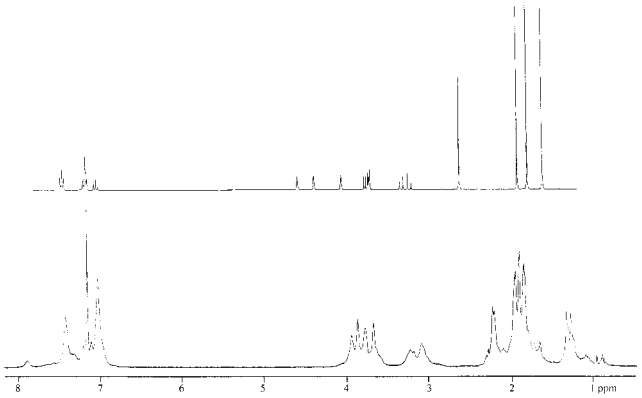

Figure 7. 400-MHz ^{1}H NMR (C_6D_6) of monomer **8a** (top) and polymer **11** (bottom).

Cyclic voltammetric studies of **11** (in a 0.1 M $[NBu_4][PF_6]$ solution in CH_2Cl_2) revealed the presence of a chemically reversible redox couple centered at $E_{1/2} = -287$ mV (versus the ferrocene/ferrocenium redox couple). The observed redox wave was quite broad, which may be attributed to a small amount of electronic communication occurring between neighboring iron centers. Interestingly, the redox couple for **11** was found centered at a significantly more negative potential (versus ferrocene/ferrocenium) compared to the monomer **8a** ($E_{1/2}$ = −133 mV).

Attempts to determine the molecular weight of **11** with GPC were unsuccessful as the polymer was found to adsorb to the styragel columns. Previous work in our group has shown that polyferrocenylphosphines, **2** (M = Fe, ER_x = PPh, R′ = H), require treatment with S_8 to give the corresponding phosphine sulfide in order to elute from the GPC columns.[48] Samples of **11** in CH_2Cl_2 were therefore treated with excess S_8 for 24 h prior to analysis by GPC (Scheme 1). ^{31}P NMR analysis of the resulting sulfurized species, **12**, revealed a downfield shift of the singlet resonance to 39.5 ppm as expected.[48] GPC analysis of a THF solution of **12** showed this material to possess a M_w value of 1.2×10^4 g·mol^{-1} with a polydispersity index (PDI) of 1.6.

To investigate whether **8a** undergoes ROP in the presence of anionic initiators, samples of **8a** were treated with equimolar amounts of ^{n}BuLi. Even after 48 h at 60 °C, no evidence for ring-opening reactions was apparent by ^{1}H NMR, which revealed only the presence of unreacted **8a**.

Previous work on phosphorus-bridged [1]ferrocenophanes has shown that these materials act as phosphine ligands for a variety of transition metals.[20] For this reason, the transition metal catalyzed ROP of **8a** was not investigated.[49] We have shown that treatment of the phosphorus-bridged [1]ferrocenophane (**1**, M = Fe, ER_x = PPh, R′ = H) with CF_3SO_3Me results in methylation of the phosphorus atom of the bridging moiety.[20,46]

(48) (a) Honeyman, C. H.; Foucher, D. A.; Dahmen, F. Y.; Rulkens, R.; Lough, A. J.; Manners, I. *Organometallics* **1995**, *14*, 5503. (b) Peckham, T. J.; Massey, J. A.; Honeyman, C. H.; Manners, I. *Macromolecules* **1999**, *32*, 2830.

(49) The coordination chemistry of **8a** and **8b** will be published elsewhere. Allen, D.; Resendes, R.; Crudden, C.; Manners, I. Unpublished results.

Scheme 2

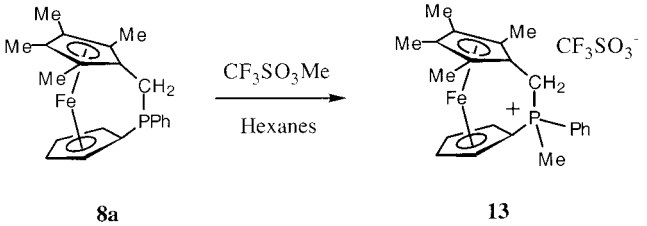

8a **13**

However, previous work by Yamashita et al. has shown that treatment of certain phosphorus(III)-containing heterocycles with methylating agents such as MeI results in cationically induced ROP.[50] To examine whether **8a** would undergo ROP under the influence of cationic initiators, samples of this species in CH_2Cl_2 were treated with 5 mol % of CF_3SO_3Me. Analysis of the reaction mixture by ^1H NMR after 24 h did not support ROP but instead suggested that partial methylation of the bridging phosphorus atom had occurred. To isolate the product, samples of **8a** in CH_2Cl_2 were treated with equimolar amounts of CF_3SO_3Me. Analysis of the reaction mixture by ^1H NMR after 24 h suggested the formation of a stable product, **13** (Scheme 2). To circumvent problems with small amounts of oxidation of the ferrocene groups, subsequent methylation reactions were conducted in hexanes in which **13** is completely insoluble. Characterization of **13** was achieved by ^1H, ^{13}C, ^{19}F, and ^{31}P NMR. Of note in the ^{31}P NMR spectrum of **13** (in C_6D_6) is the significantly downfield shifted phosphorus resonance occurring at 48.3 ppm (cf. **8a**, $\delta(^{31}P) = 7.5$ ppm), which is similar to that for the analogous phosphonium-bridged [1]ferrocenophane **1** (M = Fe, ER_x = [PMePh][CF_3SO_3], R′ = H and $\delta(^{31}P, C_6D_6) =$ 37.5 ppm).[46] The UV/visible spectrum of **13** (in THF) revealed a blue shifted λ_{max} compared to the unmethylated analogue **8a** (for **13**, $\lambda_{max} = 465$ nm, $\epsilon = 120$ M^{-1} cm^{-1}; for **8a**, $\lambda_{max} = 472$ nm, $\epsilon = 282$ M^{-1} cm^{-1}), which suggested a smaller α angle in the former species. Cyclic voltammetric studies of **13** (in a 0.1 M [NBu_4][PF_6] solution in CH_2Cl_2) revealed the presence of a chemically reversible redox couple centered at $E_{1/2} = 370$ mV (versus the ferrocene/ferrocenium redox couple). The observed redox wave for **13** was found centered at a significantly more positive potential compared to compound **8a** ($E_{1/2} = -133$ mV), consistent with the presence of a cationic bridging moiety in the former species.

Compound **13** was found to be resistant to thermal ROP, which suggested that this species possesses significantly less ring strain than the unmethylated analogue **8a**. In addition, unlike the [1]ferrocenophane analogue,[46] **13** was found to be resistant to transition metal catalyzed ROP in the presence of $PtCl_2$ or Karstedt's catalyst. To further understand these observations, an X-ray structural analysis was performed on single crystals of **13** obtained through low-temperature recrystallization. The molecular structure of **13** is shown in Figure 8. Selected structural parameters and comparative bond angles are given in Tables 2 and 3, respectively.

Of particular note in the structure of **13** is the significantly diminished α angle (for **13**, α = 11.4(7)°; cf. **8a**, α = 14.9(3)°). The observed decrease in the α angle is a result of the phosphorus atom of the bridging moiety adopting a more pronounced tetrahedral environment on methylation. Specifically, the ipso-Cp−P−CH_2 angle of **8a** increases from a value of 100.0(2)° to 110.0(2)° for **13**, consistent with the bond angle changes known to accompany the rehybridization of trigonal pyramidal phosphorus(III) centers (as found in **8a**) to pseudo-

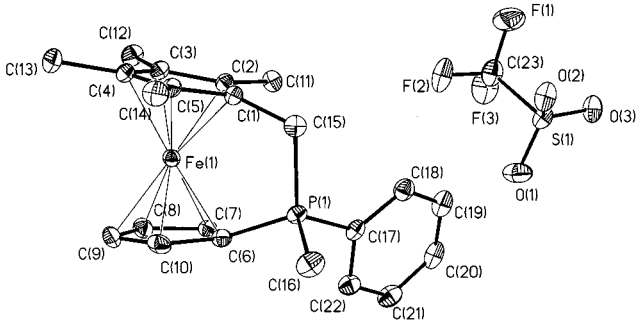

Figure 8. Molecular structure of **13** showing 30% thermal ellipsoids.

tetrahedral phosphonium centers.[51] The average β angle is also slightly (ca. 2°) larger in **13**. It is noteworthy that similar structural changes were observed on methylation of the phosphorus-bridged [1]ferrocenophane **1** (M = Fe, ER_x = PPh, R′ = H) with CF_3SO_3Me to yield the analogue **1** (M = Fe, ER_x = [PMePh][CF_3SO_3], R′ = H).[46] The resistance of **13** to polymerization is consistent with the inability of **7** to undergo ROP as this species possesses a similar α angle (for **7**, α = 11.8(1)°). Furthermore, an additional consequence of the methylation of **8a** is an increase of the steric crowding around the phosphorus center that would also be expected to make ROP less favorable. As ΔH_{ROP} for **8a** is small, for **13** the reduced tilt and increased steric bulk probably act in combination to make ROP thermodynamically unfavorable.

(iii) Polymerization Behavior of the [2]Carbothiaferrocenophane 9: The Discovery of Cationic ROP Processes. Our studies of the polymerization behavior of **7** and **8a** suggest the apparent existence of an approximate minimum α angle, between 11.8° and 14.9°, which needs to be present in the C−E bridged [2]ferrocenophane structure for ROP to occur. This notion of a minimum α angle requirement is further illustrated by the inability of **13** to undergo ROP compared to **8a**. With this in mind, the polymerization behavior of **9** was studied under a variety of conditions.

DSC analysis of **9** revealed an endotherm associated with the melting point at 68 °C and an exotherm attributed to ROP at 210 °C ($\Delta H_{ROP} = -13 \pm 5$ kJ·mol^{-1}) (Figure 6c). When a sample of **9** was heated in a sealed, evacuated Pyrex tube at 200 °C, a yellow, fibrous material was obtained that was mainly insoluble in common organic solvents. A small fraction, which was soluble in C_6D_6, was shown to be the ring-opened polycarbothiaferrocene **14** by ^1H NMR. GPC analysis of this soluble fraction (in THF) revealed a M_w of ca. 6000 g·mol^{-1} with a PDI value of 1.1.

Samples of **9** in C_6D_6 did not undergo ROP in the presence of anionic initiators such as ^{n}BuLi or transition metal precatalysts such as $PtCl_2$ or Karstedt's catalyst. However, treatment of both CH_2Cl_2 and C_6D_6 solutions of **9** with 5 mol % of the well-known cationic initiator[52−54] CF_3SO_3Me resulted in an immediate color change from bright red to light orange, followed by the precipitation of a fine yellow powder that was essentially insoluble in common organic solvents. ^1H NMR analysis of the soluble fraction demonstrated that cationic ROP to yield **14** had indeed occurred (Scheme 3).[55] Of note in the ^1H NMR spectrum

(50) Kawakami, Y.; Miyota, K.; Yamashita, Y. *Polym. J.* **1975**, *11*, 175.
(51) Cristau, H. J.; Plénat, F. *The Chemistry of Organophosphorus Compounds*; Wiley: Toronto, 1994; Vol. 3.
(52) Matyjaszewski, K. *Adv. Polym. Sci.* **1980**, *37*, 1.
(53) Matyjaszewski, K. *Adv. Polym. Sci.* **1985**, *68/69*, 186.
(54) Wagner, P. A.; Benson, J. H. *Encyclopedia of Polymer Science and Engineering*; Wiley: New York, 1989; Vol. 16.
(55) Preliminary communication: Resendes, R.; Nguyen, P.; Lough, A. J.; Manners, I. *Chem. Commun.* **1998**, 1001.

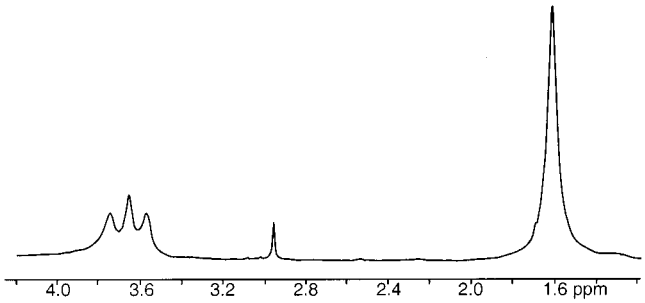

Figure 9. 400-MHz ^{1}H NMR (C_6D_6) of the soluble fraction of **14**. The resonance at 2.95 ppm is assigned to CF_3SO_3Me.

Scheme 3

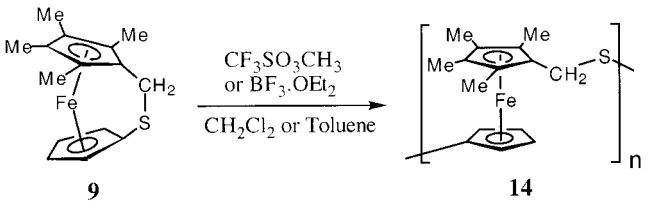

of **14** is the broad multiplet centered at 3.65 ppm that arises from both the Cp and bridging methylene protons as well as the broad resonance centered at 1.61 ppm corresponding to the Cp′ methyl protons (Figure 9).

A side reaction with the CF_3SO_3Me-initiated ROP involved oxidation of the ferrocene groups. In an attempt to circumvent this problem, initiation was attempted with the alternative Lewis acid, $BF_3{\cdot}Et_2O$. Indeed, when a toluene solution of **9** was treated with 5 mol % of $BF_3{\cdot}Et_2O$, ROP did occur, as shown by ^{1}H NMR, the immediate color change of the solution, and the precipitation of **14**. However, unlike the CF_3SO_3Me-initiated polymerization, no oxidation of the polymer was apparent. ^{1}H NMR analysis of the soluble fraction and CP-MAS ^{13}C NMR analysis of the bulk material confirmed the identity of the product as **14**. In addition, analysis by pyrolysis mass spectrometry revealed peaks which could be assigned to species possessing oligomeric $[(\eta\text{-}C_5Me_4)Fe(\eta\text{-}C_5H_4)CH_2S]_x$ units where $x = 1-3$. This again is consistent with the proposed polymeric structure of **14**. DSC analysis of **14** revealed a glass transition temperature (T_g) at ca. 60 °C. Powder X-ray diffraction studies of **14** revealed the presence of discrete reflections from values of 2θ ranging from 10° to 70° corresponding to average *d* spacings of 6.91, 5.86, and 5.28 Å. The presence of crystallinity accounts for the lack of solubility exhibited by **14** and is consistent with previous observations made for the polyferrocenylethylene **4a**.[30,36] Thermogravimetric analysis of **14** showed this material to be thermally stable up to 260 °C with 10% mass loss (T_{10}) and 50% mass loss (T_{50}) apparent at 270 and 420 °C, respectively. The thermal stability therefore appears slightly lower than that for polyferrocenylsilanes **2** (M = Fe, E = Si) (T_{10} = 400−500 °C, T_{50} = 500−900 °C).[10]

The aforementioned polymerizations of **9** represent the first examples of cationic ROP processes for a transition metal-containing heterocycle. To probe the mechanism for this novel polymerization, samples of **9** were treated with excess CF_3SO_3Me in an attempt to isolate an intermediate such as a cationic *S*-methylated derivative or a ring-opened analogue. With the same goal in mind, samples of **9** were slowly added to excess CF_3SO_3Me. In both cases only polymer **14** was formed, which suggested that the propagation step of the ROP reaction occurs much more rapidly than the initial methylation. Similarly, treatment of **9** with excess CF_3SO_3Me in the presence of

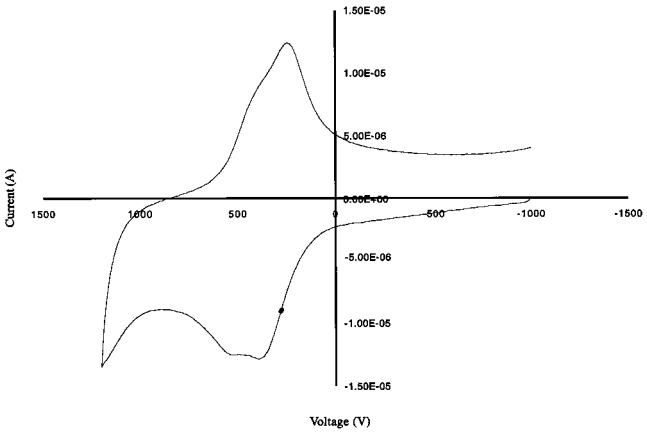

Figure 10. Cyclic voltammagram of **14** in CH_2Cl_2 (0.1 M NBu_4PF_6 supporting electrolyte, scan rate 250 mV/s).

Scheme 4

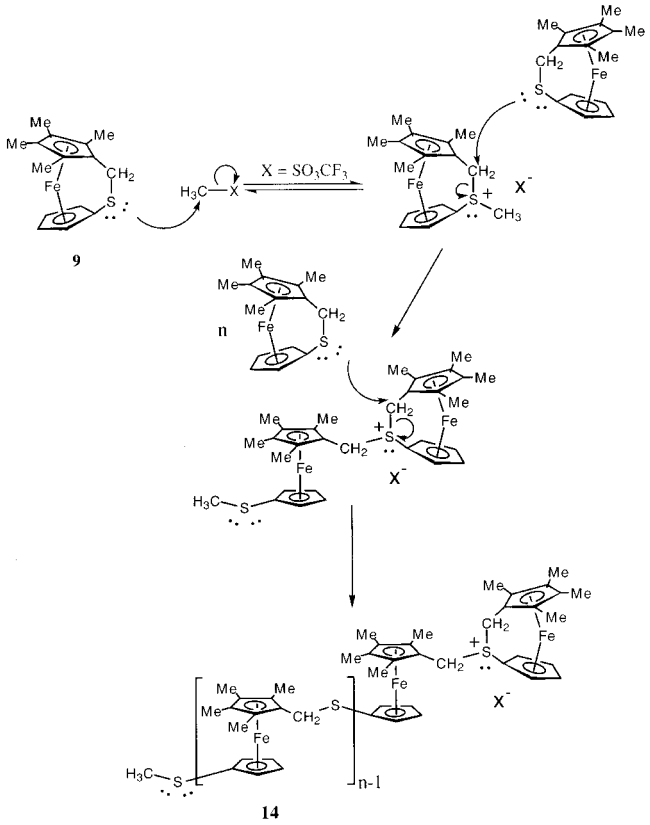

$Li[O_3SCF_3]$ or with 10 mol % of CF_3SO_3Me in the presence of 1 equiv of $[NBu_4]Cl$ also failed to allow the detection or isolation of any ring-opened intermediates.

Treatment of **9** with equimolar amounts of $BF_3{\cdot}Et_2O$ in the presence of excess 2,6-di-*tert*-butylpyridine as a selective proton trap resulted in complete inhibition of the ROP process as shown by ^{1}H NMR. This observation suggests that the cationic ROP of **9** in the presence of $BF_3{\cdot}Et_2O$ relies on protonation of **9** from trace amounts of HF or $H[BF_3(OH)]$ in solution. In contrast, treatment of **9** with equimolar amounts of CF_3SO_3Me in the presence of excess 2,6-di-*tert*-butylpyridine was not found to prevent ROP, which indicated that in this case the initiation step for the cationic ROP of **9** involves methylation. A tentative mechanism that is consistent with these results is shown in Scheme 4.

Cyclic voltammetric studies on soluble fractions of **14** in a 0.1 M $[NBu_4][PF_6]$ solution in CH_2Cl_2 revealed the presence

Scheme 5

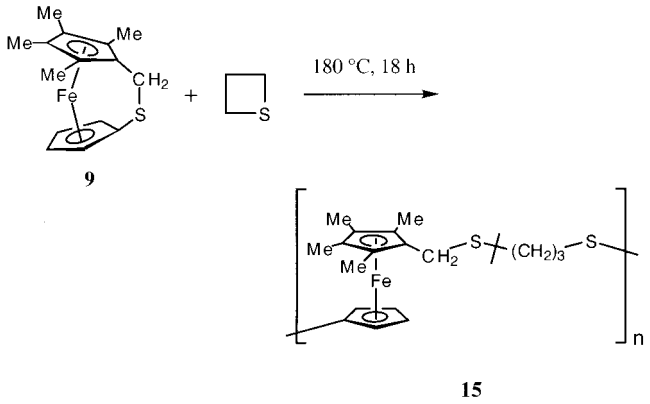

of two chemically reversible redox waves with a redox coupling, $\Delta E_{1/2}$, of ca. 140 mV (Figure 10). While this value is not as high as that detected in ring-opened polyferrocenes with a single atom spacer (**2**) (typically $\Delta E_{1/2} = 200-320$ mV), it is significantly larger than the 90 mV coupling detected for polyferrocenylethylene **4b**. Even though the overall length of the diatomic bridging moiety (and hence Fe···Fe distance) is larger in **14** than in **4b**, owing to the larger covalent radius of sulfur compared to carbon (r_{cov}(C) = 0.77 Å versus r_{cov}(S) = 1.04 Å),[37] the apparent increase in electronic interaction between adjacent Fe centers may be attributable to the enhanced polarizability of sulfur compared to carbon. This is consistent with observations made for ring-opened [1]ferrocenophanes and their corresponding model oligomers where the electronic interaction is more dependent on the nature of the bridging unit than on the average intramolecular Fe···Fe distance.[24]

(iv) Copolymerization Behavior of the [2]Carbothiaferrocenophane 9 with Other Oxygen- and Sulfur-Containing Heterocycles. In an attempt to generate soluble analogues of **14**, copolymerization reactions were investigated. To this end, several oxygen- and sulfur-containing heterocycles such as THF, oxetane ($(CH_2)_3O$), propylene oxide ($MeCHCH_2O$), ethylene oxide ($(CH_2)_2O$), tetrahydrothiophene ($(CH_2)_4S$), and trimethylene sulfide ($(CH_2)_3S$) were investigated as potential comonomers in the cationic ROP of **9**. In all cases, where equimolar amounts of each monomer and 2:1 mole ratios of **9**:heterocycle were used, the $BF_3{\cdot}Et_2O$ initiated cationic ROP resulted only in the corresponding homopolymers as shown by ^{1}H NMR. However, when samples of **9** and $(CH_2)_3S$ were heated in an evacuated and sealed Pyrex tube at 180 °C for 18 h, the random copolymer, **15**, was obtained (Scheme 5).

Polymer **15** was found to be completely soluble in polar organic solvents and the weight average molecular weight (M_w) was determined by GPC in THF to be 3.0×10^5 g·mol^{-1} with a polydispersity index (PDI) of 2.6. ^{1}H NMR, ^{13}C NMR, and pyrolysis MS confirmed the structure of **15** to be that depicted in Scheme 5. Of note in the ^{1}H NMR of **15** are the broad resonances centered at 1.74, 2.42, and 3.60 ppm, which correspond to the C_5Me_4, $(CH_2)_3S$, and C_5H_4/CH_2 protons, respectively. ^{13}C NMR analysis of **15** reveals peaks consistent with the proposed structure of **15**, and switching groups between the different segments (34.3−37.4 ppm) are apparent. Given that homopolymer **14** is essentially insoluble in common organic solvents and that the presence of ^{1}H and ^{13}C NMR resonances due to the [(η-C_5Me_4)Fe(η-C_5H_4)CH_2S] segments was detected, the evidence is convincing in support of a random copolymer structure for **15** rather than the alternative possibility, that the material isolated is simply a mechanical blend of the two homopolymers **14** and $[(CH_2)_3S]_n$. Pyrolysis MS also provided convincing support for a random copolymer for **15** as peaks which correspond to molecular fragments of the type [(η-C_5Me_4)Fe(η-C_5H_4)$CH_2S]_x$[$(CH_2)_3S]_y$ ($x = 1-4$, $y = 1-8$) were detected (Figure 11). The UV/visible spectrum of **15** (in THF) in the region of 400−800 nm showed an absorption at 436 nm (ϵ = 124 M^{-1} cm^{-1}) that was assigned to the lowest energy d−d transition for the [(η-C_5Me_4)Fe(η-C_5H_4)CH_2S] repeat units of **15**. The shift in λ_{max} to a shorter wavelength, compared to that observed for **9** (λ_{max} = 475 nm), is once again consistent with the relief in ring strain accompanying the ROP of **9**. Thermogravimetric analysis of **15** demonstrated this material to be more thermally stable than **14** with significant mass loss detected at >300 °C (for **15**, T_{10} = 320 °C, T_{50} = 400 °C).

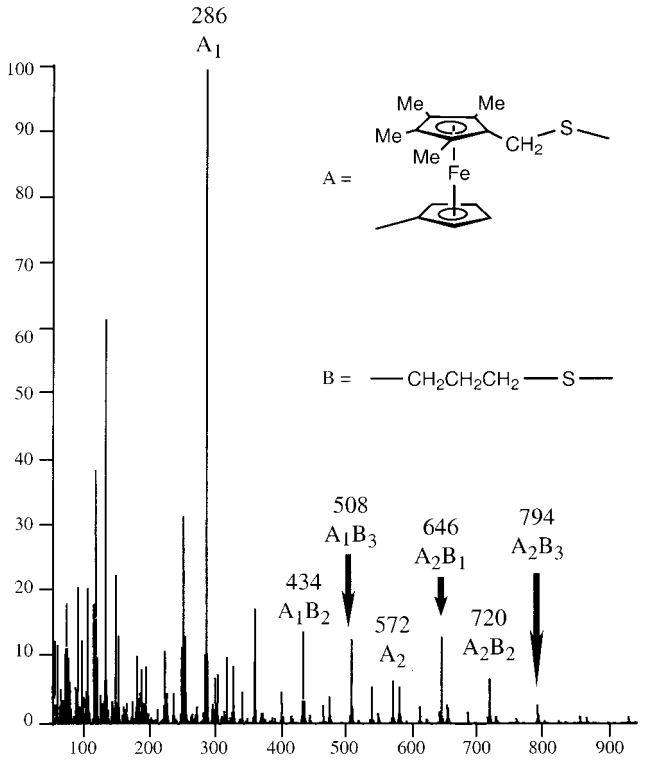

Figure 11. Pyrolysis MS of **15**. Peaks corresponding to random oligomeric units of **15** are highlighted.

Summary

The incorporation of different elements into the C−E bridged [2]ferrocenophane framework has allowed tuning of the overall ring strain and thus polymerizability. The least strained of these species with a C−Si bridge (**7**, $\alpha = 11.8(1)°$) was found to be completely resistant to ROP under all conditions studied. The significantly more strained species with C−P and C−S bridges (**8a**, $\alpha = 14.9(3)°$; and **9**, $\alpha = 18.5(1)°$) were both found to undergo ROP reactions.[56,57] These polymerizations were found to possess very small ΔH_{ROP} values (ca. −10 to −20 kJ mol^{-1})

(56) The bond strengths for C−Si, C−P, and C−S bonds are not substantially different (301, 264, and 272 kJ mol^{-1}: Cotton, F. A.; Wilkinson, G. *Basic Inorganic Chemistry*, 3rd ed.; Wiley: New York, 1995; p 12) and are unlikely to explain any kinetic differences in polymerizability. We have previously shown that Si-bridged [1]ferrocenophanes undergo thermal ROP via a C−Si bond cleavage mechanism at temperatures as low as 130 °C and our unsuccessful attempts to induce the thermal ROP of **7** were performed at temperatures as high as 350 °C. See: Pudelski, J. K.; Manners, I. *J. Am. Chem. Soc.* **1995**, *117*, 7265 and ref 3.

(57) The mechanism for the thermal ROP of ferrocenophanes is not known with certainty but a heterolytic mechanism involving initiation by trace quantities of nucleophilic impurities is plausible. See: Jäkle, F.; Rulkens, R.; Zech, G.; Massey, J. A.; Manners, I. *J. Am. Chem. Soc.* **2000**, *122*, 4231.

that are substantially less than those found for [1]ferrocenophanes which are significantly more strained ($\Delta H_{ROP} = -36$ to -130 kJ mol^{-1}).[21,28,44] Indeed, the methylated analogue of **8a**, the phosphonium species **13**, ($\alpha = 11.4(7)°$), possesses a slightly less strained structure than that of **8a** ($\alpha = 14.9(3)°$) and was shown to be resistant to ROP. As previous theoretical work has indicated that the tilt-angle α plays a key role in determining the polymerizability of ferrocenophanes,[21,22] the findings of this study therefore suggest that for the [2]ferrocenophane systems investigated, an approximate minimum α angle may exist between 11.8° and 14.9°, below which ROP will not occur. Significantly, ROP of the C−S bridged species **9** in the presence of CF_3SO_3Me or $BF_3{\cdot}Et_2O$ represents the first example of the cationic polymerization of a transition metal-containing heterocycle. The resulting polymer, **14**, possesses significant Fe···Fe interactions which appear more substantial than those present in analogues with CH_2-CH_2 spacers for which the Fe···Fe distance should be smaller. This emphasizes the dominant influence of the electronic nature of the spacer on the metal−metal interactions present in ring-opened polymetallocenes. We are currently exploring the preparation of more soluble analogues of **14** to perform detailed studies of the physical properties of such materials.

Acknowledgment. This research was supported by the Petroleum Research Fund, administered by the American Chemical Society. R.R. is grateful to the Natural Sciences and Engineering Research Council of Canada (NSERC) for a postgraduate scholarship and F.J. is grateful to the D.F.G. for a postdoctoral fellowship. In addition, I.M. thanks NSERC for an E. W. R. Steacie Fellowship (1997−99), the University of Toronto for a McLean Fellowship (1997−2003), and the Ontario Government for a PREA award (1999). Additional thanks go to Prof. A. Yudin for use of the electrochemical equipment and M. Mamak for WAXS measurements.

Supporting Information Available: Text describing synthetic procedures and all crystal data for **7**−**9** and **13** (PDF). This material is available free of charge via the Internet at http://pubs.acs.org.

JA002750E